

# Distribution and Determinants of Eye Size and Shape in Newborn Children: A Magnetic Resonance Imaging Analysis

Laurence Shen Lim,<sup>1</sup> Gim Hong Chong,<sup>2</sup> Pei Ting Tan,<sup>3</sup> Yap-Seng Chong,<sup>4</sup> Kenneth Kwek,<sup>5</sup> Peter D. Gluckman,<sup>6,7</sup> Marielle V. Fortier,<sup>8</sup> Seang-Mei Saw,<sup>9</sup> and Anqi Qiu<sup>2,6,10</sup>

<sup>1</sup>Singapore Eye Research Institute, Singapore

<sup>2</sup>Department of Bioengineering, National University of Singapore, Singapore

<sup>3</sup>Biostatistics Unit, Yong Loo Lin School of Medicine, National University of Singapore, National University Health System, Singapore

<sup>4</sup>Department of Obstetrics & Gynaecology, Yong Loo Lin School of Medicine, National University of Singapore, National University Health System, Singapore

<sup>5</sup>Department of Maternal Fetal Medicine, KK Women's and Children's Hospital, Singapore

<sup>6</sup>Singapore Institute for Clinical Sciences, the Agency for Science, Technology and Research, Singapore

<sup>7</sup>Liggins Institute, University of Auckland, Auckland, New Zealand

<sup>8</sup>KK Women's and Children's Hospital, Singapore

<sup>9</sup>Saw Swee Hock School of Public Health, National University of Singapore, Singapore

<sup>10</sup>Clinical Imaging Research Center, National University of Singapore, Singapore

Correspondence: Seang-Mei Saw, Saw Swee Hock School of Public Health and Yong Loo Lin School of Medicine, National University of Singapore, 16 Medical Drive (MD3), Singapore 117597; seang\_mei\_saw@nus.edu.sg. Anqi Qiu, Department of Bioengineering, National University of Singapore, 9 Engineering Drive 1, Block EA #03-12, Singapore 117576; bieqa@nus.edu.sg.

Submitted: August 6, 2012

Accepted: May 17, 2013

Citation: Lim LS, Chong GH, Tan PT, et al. Distribution and determinants of eye size and shape in newborn children: a magnetic resonance imaging analysis. *Invest Ophthalmol Vis Sci*. 2013;54:4791-4797. DOI:10.1167/iovs.12-10713

**PURPOSE.** To determine the eye size and shape obtained by magnetic resonance imaging (MRI), and to determine associations with antenatal factors in newborn children.

**METHODS.** A subset of 173 full-term newborn children from the Growing Up in Singapore Towards Healthy Outcomes (GUSTO) birth cohort underwent MRI. Eye volume and surface area were measured. Eye shape was assessed qualitatively from three-dimensional models, and quantitatively by measurement of longitudinal axial length (AL, the length from the posterior corneal surface to the retinal surface), and horizontal width and vertical height of the internal eye along the cardinal axes. Oblateness was calculated as  $1 - (AL/\text{width})$  or  $1 - (AL/\text{height})$ . Oblate eyes had oblateness  $> +0.01$ , spherical eyes had oblateness between  $+0.01$  and  $-0.01$ , and prolate eyes had oblateness  $< -0.01$ .

**RESULTS.** A total of 346 eyes of 173 children were included. Mean oblateness using width was  $-0.06 \pm 0.05$  (range,  $-0.23$  to  $+0.08$ ), and mean oblateness using height was  $-0.01 \pm 0.04$  (range,  $-0.19$  to  $+0.13$ ). Using width, most eyes were prolate (294 eyes, 85%); and using height, the largest proportion of eyes was prolate (163 eyes, 47%). Eyes with longer ALs had greater widths, heights, volumes, and surface areas than eyes with shorter ALs ( $P < 0.001$  for all). With increasing AL, eyes became increasingly prolate. Children of less educated mothers had longer ALs ( $P = 0.02$ ). Malay children had larger eye volumes and surface areas than Chinese or Indian children.

**CONCLUSIONS.** Most newborn Singaporean Asian children are born with prolate eyes. A longitudinal study is required to determine if globe shape at birth influences subsequent refractive changes.

Keywords: myopia, magnetic resonance imaging, neonates, image analysis

Myopia is an increasingly important public health problem, with particularly high rates amongst Chinese East Asian populations such as those in Taiwan and Singapore.<sup>1-3</sup> Understanding the pathogenesis of myopia is important for formulating prevention strategies. Pathological myopia is associated with potentially blinding complications such as retinal detachment, choroidal neovascularization, and macular holes,<sup>4-6</sup> and even less severe forms of myopia predispose to glaucoma and cataract in adulthood.<sup>7,8</sup> Furthermore, the lifetime socioeconomic costs of myopia are considerable.<sup>9-11</sup>

Several risk factors for myopia in children have been identified in large-scale epidemiologic studies. These include a genetic basis for myopia susceptibility,<sup>12,13</sup> and a diverse range

of environmental factors such as near-work, outdoor activity, socioeconomic background, and nutrition.<sup>14-19</sup> However, the pathogenetic mechanisms underlying myopia development remain poorly understood, with the relative contributions of genetic and environmental influences a key point of contention.

Myopia has traditionally been regarded as a mismatch between the refractive power of the eye and the length of the eyeball. However, it is increasingly being recognized that the anatomical deviations in myopia involve more complex three-dimensional (3D) changes than are captured in a single-dimension axial measurement.<sup>20-25</sup> The shape of the eyeball is a variable that is increasingly being investigated with the advent

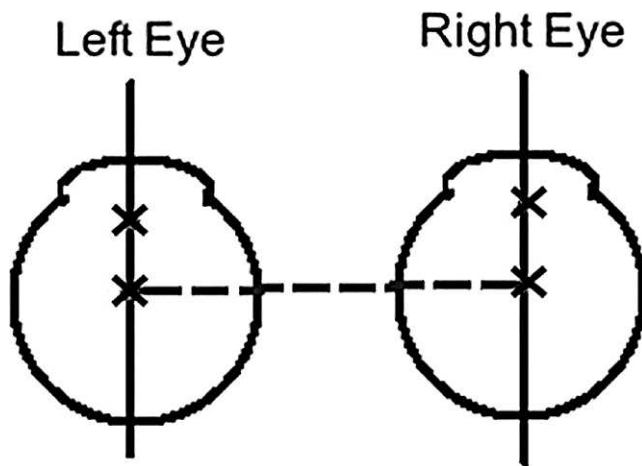


**FIGURE 1.** Diagram illustrating the method by which the axes of the eyes were determined. Two spherical models were first used to fit the corneal and vitreous chamber boundaries delineated in the MR images. The crosses represent the centers of the two fitted spheres. The solid lines passing through the two crosses in each eye were defined as the longitudinal axes of each eye. A line was then drawn to connect the centers of the left and right eyes (dashed line). The line perpendicular to the plane composed of the solid and dashed lines was defined as the vertical axis of the eye. Finally, the line perpendicular to the solid line on the plane composed of the solid and dashed lines, was defined as the horizontal axis of the eye.

of high-resolution in vivo imaging techniques such as magnetic resonance imaging (MRI) and computer software for three-dimensional modeling. We have previously shown that the internal eye surface area increases with myopia in young children. Eye shape is different in myopic eyes compared to non-myopic eyes, even in its early stages. In myopic eyes, more myopic refraction is associated with an increasingly prolate shape due to greater axial elongation. In non-myopic eyes, more myopic or less hyperopic refraction is associated with roughly equal increases in length, width and height, indicating generalized enlargement of the globe.<sup>24</sup> However, some basic questions concerning the variation of human eye shape remain unanswered.

There are no data on the distribution and variability of ocular dimensions and shape in the normal infant. Evaluating ocular dimensions and shape in infancy provides information on the baseline shape of the globe, before any environmental stimuli can have an effect. Race and a parental history of myopia have been associated with eye size and growth in children, but it is not known if these factors are correlated with ocular dimensions and shape at birth.<sup>26-30</sup>

The aims of this study are to determine the range and distribution of measures of eye size and shape, and to determine the associations between race and parental myopia with eye dimensions and shape, in newborn children.

## METHODS

This study was conducted on a subset of the birth cohort study termed GUSTO: Growing Up in Singapore Towards Healthy Outcomes. This is Singapore's largest and most comprehensive birth cohort study and is designed to adopt a life course approach to define the importance of fetal and developmental factors in early pathways to metabolic diseases.

The study population consists of the children of all pregnant women aged 18 years and above attending the first trimester antenatal dating ultrasound scan clinic at the two major public maternity units, namely National University

Hospital (NUH) and KK Women's and Children's Hospital (KKH), in Singapore. These subjects are Singapore citizens or permanent residents who are Chinese, Malay, or Indian with homogenous parental ethnic background and have the intention to eventually deliver in NUH or KKH and to reside in Singapore for the next 5 years. Mothers on chemotherapy, psychotropic drugs, or with Type I Diabetes Mellitus were excluded. Only women who agreed to donate birth tissues such as cord, placenta, and cord blood at delivery were included. Out of the 3335 screened, 1163 (62% of the eligibles screened) pregnant women were recruited from June 2009 to September 2010.

A key feature of the GUSTO study is to have body fat measures on all participants. After delivery, the children of enrolled subjects underwent whole body MRI, including brain imaging, at 5 to 17 days to accurately document body fat.

Written informed consent from the parents of subjects was obtained. Most of the children had returned home by the time of the MRI, and many parents were unwilling to return to the hospital for the scan. Also, as we did not sedate the babies, many children who were unable to sleep through the scan had to be excluded. As such, only approximately 15% of the total cohort provided data for this study.

The study was approved by the Centralized Institutional Review Boards of the Singapore Health Services and Domain Specific Review Board (DSRB) of National Health Care Group.

## MRI Acquisition and Eye Shape Analysis

**Data Acquisition.** At 5 to 17 days of life, neonates underwent fast spin-echo T2-weighted MRI (TR = 3500 ms; TE = 110 ms; field of view [FOV] = 256 mm × 256 mm; matrix size = 256 × 256; 50 axial slices with 2.0-mm thickness) scans using a 1.5-Tesla GE scanner (Signa 1.5T MR; GE Healthcare, Milwaukee, WI) with an 8-channel head coil at the Department of Diagnostic and Interventional Imaging of the KKH. Two T2-weighted images were acquired per subject. The image resolution was 1 × 1 × 2 mm<sup>3</sup>. The scans were acquired when subjects were sleeping in the scanner. No sedation was used and precautions were taken to reduce exposure to the MRI scanner noise. A neonatologist was present during each scan. A pulse oximeter was used to monitor heart rate and oxygen saturation throughout the entire scans. One-hundred eighty nine neonates underwent the T2-weighted MRI scans. Through visual inspection, 173 neonates with at least one good T2-weighted MRI scan were included in the analyses.

**Segmentation.** We developed an atlas-based segmentation approach to automatically delineate the left and right eyes from the T2-weighted image. We manually delineated the eye from one subject's image. Segmenting the eye of other subjects was a matter of extrapolating from this manually labeled training image, referred as an atlas. This method is typically referred as atlas-based segmentation. It requires the use of image registration in order to align the atlas image to the other subjects' images. We then constructed the 3-dimensional shape of the eye.<sup>31-33</sup>

**3D Eye Coordinate System.** We constructed a 3D coordinate system for each eye by determining the long, horizontal and vertical axes (Fig. 1). We fitted the eye shape using two spheres: one modeled on the corneal region and the other modeled on the vitreous humor. One sphere encompassed the whole of the corneal region and the other encompassed the whole of the vitreous chamber. We employed the least-square optimization method to fit the eyeball shape using these two spheres. The geometric center of the eye was then represented by the center of the sphere containing the vitreous humor. The long axis of the eyeball was defined as the line passing through the centers of the

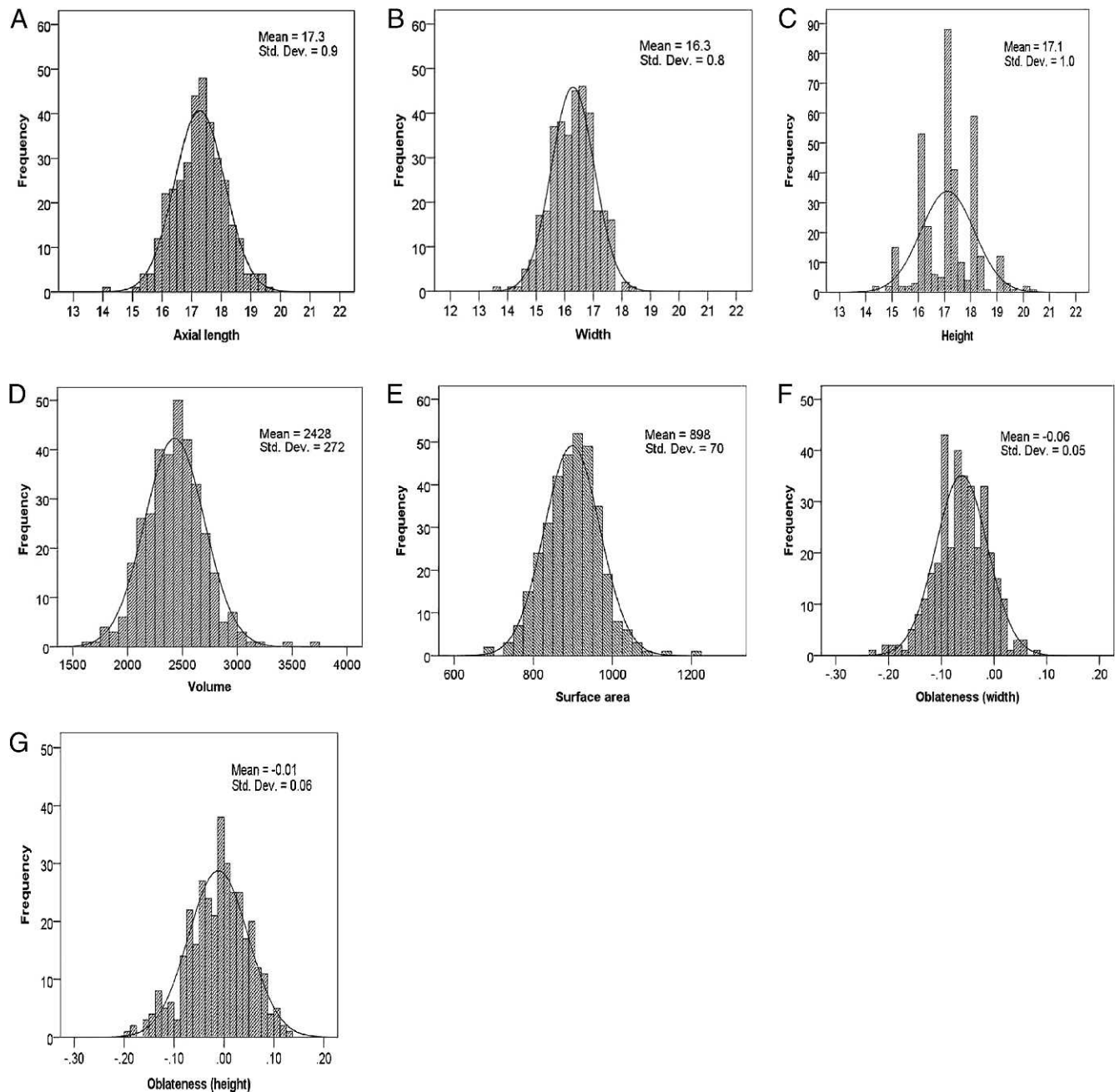


**FIGURE 2.** Distribution of globe dimensions and shape indices. (A) Distribution of globe axial length. (B) Distribution of globe width. (C) Distribution of globe height. (D) Distribution of globe volume. (E) Distribution of globe surface area. (F) Distribution of oblateness ( $1 - [AL/width]$ ). (G) Distribution of oblateness ( $1 - [AL/height]$ ).

mentioned two fitted spheres. The length, width, and height were measured automatically by the software. The traditional AL was computed as the distance between the most anterior and posterior points of the long axis, representing the length from the posterior corneal surface to the retinal surface. The vertical axis was then determined as the cross product between the long axis of the eye and the line passing through the centers of the left and right eyes. The cross product is a binary operation on two vectors in 3D space and results in a vector that is perpendicular to both of the vectors being multiplied and therefore normal to the plane containing them. The height of the eye was then calculated as the distance between the most superior and inferior points along the vertical axis. Finally, the horizontal axis of each eye was

determined as the cross product of the long and vertical axes. The width of the eye was computed as the distance between the most temporal and nasal points along the horizontal axis. The length, width, and height described above were the measurements for the internal eye.<sup>23</sup> The term “globe” in this paper refers to the internal surface of the eye.

**Eye Volume, Surface Area, and Shape Measurements.** The volume of the eye was computed as the number of voxels labeled as part of the eye in the T2-weighted image multiplied by the image resolution, and the surface area of the eyeball was approximated as the area of the triangulated mesh.

We have used these scanning and analysis techniques in a previous study on older children.<sup>24</sup> In that study, we evaluated the accuracy of the MRI segmentation by comparing the



TABLE 1. Distribution of Globe Shapes According to Oblateness Values

	Oblateness Using Width, <i>n</i> (%)	Oblateness Using Height, <i>n</i> (%)
Prolate, oblateness < -0.01	294 (85)	163 (47)
Spherical, oblateness -0.01 to +0.01	27 (8)	55 (16)
Oblate, oblateness > +0.01	25 (7)	128 (37)

longitudinal axial length obtained from MRI with the axial length using partial coherence interferometer (PCI), with no significant differences found.

### Statistical Analysis and Definitions

A summary index of eye shape was given by oblateness,<sup>34</sup> defined as  $1 - (\text{axial length}/\text{equatorial diameter})$ . Oblateness was determined using both the width and height as the equatorial diameter. A prolate eye was defined as oblateness < -0.01, while an oblate eye was defined as oblateness > +0.01. A spherical eye was defined as oblateness between -0.01 and +0.01.

The normality of the distributions of the various ocular parameters was assessed by plotting histograms and Q-Q plots, calculating skewness and kurtosis, and with formal tests of normality, including the Komolgorov-Smirnov one sample test. Mixed linear models were constructed to account for intereye correlations, with AL as the dependent variable and the other ocular measurements as the independent variables, with adjustments for mother's race, mother's age, mother's education, gestational age, birth weight, birth length, and parental myopia.<sup>19,27,35</sup> Additional models were constructed with the ocular measurements as the dependent variables and antenatal factors as independent variables, adjusted for the same covariates as appropriate. Descriptive statistics was presented as the mean ( $\pm$ standard deviation). All probabilities quoted were two-sided and all statistical analyses were undertaken using (SPSS 20.0; IBM Corporation, Armonk, NY).

### RESULTS

A total of 346 eyes of 173 newborn children (5-17 days old) were included in the analyses. The mean gestational age at the time of MRI examination was  $38.4 \pm 1.1$  weeks and the mean birth weight was  $3125 \pm 409$  g.

Measurements were obtained from all the MR images. The mean AL, width, and height were  $17.3 \pm \text{SD } 0.9$  mm (range, 14.0-19.6),  $16.3 \pm 0.8$  mm (13.7-18.4); and  $17.1 \pm 1.0$  mm (14.3-20.3), respectively, while the mean volume and surface area of the globe were  $2428 \pm 272$  mm<sup>3</sup> (1653-3744) and  $898 \pm 70$  mm<sup>2</sup> (677-1217), respectively. The mean oblateness in relation to width was  $-0.06 \pm 0.05$  (-0.23 to 0.08), and the mean oblateness in relation to height was  $-0.01 \pm 0.04$  (-0.19 to +0.13).

TABLE 2. Associations Between AL and Width, Height, Volume, Surface Area, and Shape of the Globe

AL in Quartiles	Volume (SD)	Width (SD)	Height (SD)	Surface Area (SD)	Oblateness, $1 - (\text{AL}/\text{width})$ (SD)	Oblateness, $1 - (\text{AL}/\text{height})$ (SD)
Q1, <i>n</i> = 86, <16.7	2154 (192)	15.7 (0.7)	16.6 (1.0)	826 (52)	-0.03 (0.05)	0.02 (0.05)
Q2, <i>n</i> = 87, 16.70-17.30	2399 (185)	16.3 (0.6)	17.0 (0.8)	889 (43)	-0.05 (0.04)	-0.001 (0.05)
Q3, <i>n</i> = 86, 17.30-17.81	2497 (170)	16.4 (0.6)	17.3 (1.0)	917 (43)	-0.07 (0.04)	-0.02 (0.06)
Q4, <i>n</i> = 87, >17.81	2659 (251)	16.7 (0.7)	17.6 (1.0)	960 (63)	-0.10 (0.05)	-0.05 (0.06)
<i>P</i> trend*	<0.001	<0.001	<0.001	<0.001	<0.001	<0.001

Values are mean (SD), min - max. *n*, number of eyes.

\* *P* trend unaffected when adjusted for race, mother's age, mother's education, gestational age, and parental myopia.

Figure 2 shows histograms of AL, width, height, volume, surface area, and oblateness. All the ocular measurements were normally distributed.

The distribution of globe shapes based on oblateness is shown in Table 1. Using width most eyes were prolate (294 eyes, 85%), and, using height, the largest proportion of eyes was also prolate (163 eyes, 47%).

Significant positive associations were found between AL and the volume, width, height, and surface area of the globe. Eyes with longer AL were likely to have greater widths, heights, volumes, and surface areas ( $P < 0.001$ ) for all. With increasing AL, eyes assumed increasingly prolate profiles using both eye width and height to calculate oblateness (Table 2). Qualitatively, eyes with the longest AL appeared prolate upon inspection of the 3D models (Fig. 3).

The associations between antenatal factors that predict myopia in later life and AL were evaluated in multivariate analyses (Table 3). Maternal education as an indicator of socioeconomic status was associated with axial length. Children of mothers with lower educational qualifications had longer axial lengths ( $P = 0.02$ ). Race was associated with eye volume and surface area. Malay children had larger eye volumes and surface areas ( $P = 0.04$  for both) compared with Chinese or Indian children, though this was of borderline significance.

### DISCUSSION

Our study provides normative data on the ocular dimensions and shape in a cohort of newborn Asian children. Measurement of ocular dimensions and shape are normally distributed. The mean AL was 17.3 mm, comparable with that reported in other studies on newborn eyes.<sup>34,36-38</sup> Axer-Seigel reported mean values of  $16.6 \pm 0.4$  mm for right eyes and  $16.5 \pm 0.4$  mm for left eyes in term infants, while Isenberg reported a mean value of 16.2 mm.<sup>37,38</sup> The mean value at term reported by Fledelius in preterm infants, adjusted for an assumed average eye elongation of 0.14 mm per week, was 17.02 mm.<sup>36</sup>

The advent of high-resolution MRI and computer software for 3D modeling has allowed for the direct study of eye shape in vivo. Cheng<sup>39</sup> found that adult myopic eyes had the same shape as hyperopic or emmetropic eyes, with the width of the whole globe longer than the AL and height. Atchison studied the shape of the retinal surface in hyperopia and myopia, and found that both emmetropic and myopic retinas were oblate in

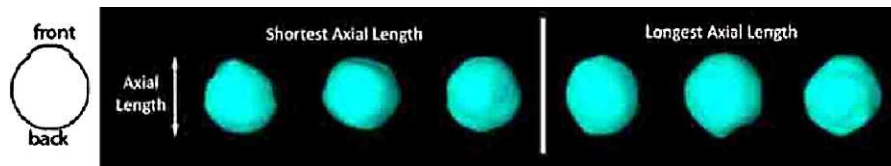


FIGURE 3. 3D models of representative eyes with the longest and shortest axial lengths.

shape.<sup>20</sup> In another analysis of the internal dimensions of the eye,<sup>21</sup> the same authors found that myopic eyes were elongated more in length but approximately equal proportions of myopic eyes fitted global expansion and axial elongation models exclusively. As described earlier, we have previously shown that axial internal globe enlargement occurs in myopic eyes leading to a prolate shape, whereas non-myopic eyes enlarge globally in length, width and height.<sup>24</sup> In this study, we have shown that the shape of the eyeball is correlated with the axial length. Eyes with longer axial lengths have increasingly prolate profiles.

Data on globe shape in very young children is scarce. Ishii reported on the shape of the globe from MRI analyses in a cohort of 105 healthy patients with ages ranging from 1 month to 19 years undergoing routine imaging.<sup>34</sup> Oblateness was calculated similarly, but a prolate shape was defined as oblateness < 0, an oblate shape as oblateness > 0, and a sphere as oblateness = 0. As in our study, AL was correlated with the oblateness of the eye. At age 0, the eyes were mostly oblate, with oblateness increasing with age. In contrast, using the same definitions of globe shape, most eyes in our study were prolate (90.2% using width to calculate oblateness, and 56.1% using height to calculate oblateness). However, the actual number of subjects with age 0 in Ishii's study was very small (approximately 10-15 subjects). Our results suggest that most children are born with prolate globes. Newborn children are however usually not myopic.<sup>40,41</sup> This suggests that, in newborn children, the other refractive components of the eye (e.g., lens) are more important determinants of refraction than eye shape. Longitudinal evaluation of the children in our cohort will allow us to determine if eye shape and size at birth are correlated with the subsequent development of ametropia.

This epidemiological association between parental myopia and myopia<sup>26,30</sup> may be due to either genetic or environmental influences, and there is still no conclusive proof of either. In the Orinda Longitudinal Study of Myopia,<sup>27</sup> Zadnik et al. performed a cross-sectional analysis of eye size and shape in relation to parental myopia in 662 nonmyopic children. After controlling for near work, children with two myopic parents had longer eyes and less hyperopic refractive errors than children with only one myopic parent or no myopic parents. However, in a study on 4468 Chinese children performed in Hong Kong using similar methodology,<sup>42</sup> although nonmyopic children with a stronger parental history of myopia tended to be less hyperopic before the onset of myopia, corresponding associations with AL did not follow the same pattern. Subsequent eye growth and the development of myopic refractive errors occurred more rapidly among children with a stronger parental history of myopia. In our study, parental myopia was not correlated with the size or shape of the eye at birth. However, we found an interesting association between lower maternal educational qualifications and longer globes in the offspring. Longitudinal evaluation to determine if these children with longer globes at birth subsequently develop myopia will help to shed light on whether myopia predisposition is congenitally determined.

Race has been associated with the prevalence of myopia in young children. In the adult population in Singapore, the Chinese have a higher prevalence of myopia than Malays and Indians.<sup>43,44</sup> In our study, Malay children had larger globes (larger volumes and surface areas) than Chinese and Indian children, though this was only of borderline significance. This contrasts with the lower prevalence of myopia in adult Malay

TABLE 3. Associations Between Antenatal Factors and Ocular Dimensions and Shape

	AL (SD)	Volume (SD)	Width (SD)	Height (SD)	Surface Area (SD)	Oblateness, 1 - (AL/width) (SD)	Oblateness, 1 - (AL/height) (SD)
<b>Race</b>							
Chinese, n = 146	17.2 (0.8)	2412 (246)	16.3 (0.7)	17.1 (1.0)	894 (65)	-0.06 (0.04)	-0.01 (0.06)
Malay, n = 150	17.3 (0.8)	2450 (278)	16.3 (0.8)	17.2 (1.0)	905 (70)	-0.06 (0.05)	-0.01 (0.06)
Indian, n = 48	17.4 (1.0)	2442 (288)	16.4 (0.8)	17.0 (1.0)	900 (72)	-0.06 (0.05)	-0.02 (0.06)
P value	0.34	0.46	0.59	0.60	0.44	0.63	0.31
Adjusted P trend*	0.11	0.04	0.31	0.27	0.04	0.81	0.25
<b>Maternal education</b>							
Primary, n = 14	17.7 (0.8)	2484 (287)	16.4 (0.7)	17.6 (1.5)	917 (72)	-0.08 (0.05)	-0.01 (0.08)
Secondary, n = 188	17.3 (0.8)	2430 (229)	16.3 (0.7)	17.1 (0.9)	900 (59)	-0.06 (0.05)	-0.01 (0.06)
Tertiary, n = 138	17.2 (0.9)	2423 (308)	16.3 (0.8)	17.1 (1.1)	896 (78)	-0.06 (0.05)	-0.01 (0.06)
P value	0.09	0.55	0.63	0.51	0.33	0.22	0.44
Adjusted P trend	0.02	0.24	0.35	0.55	0.12	0.27	0.28
<b>Parental myopia</b>							
0, n = 110	17.2 (1.0)	2412 (294)	16.2 (0.9)	17.1 (1.0)	894 (77)	-0.06 (0.05)	-0.01 (0.06)
1, n = 142	17.3 (0.8)	2433 (238)	16.4 (0.7)	17.1 (1.0)	900 (60)	-0.06 (0.05)	-0.02 (0.06)
2, n = 94	17.2 (0.8)	2440 (295)	16.2 (0.7)	17.2 (1.0)	901 (76)	-0.06 (0.04)	-0.01 (0.06)
P value	0.93	0.46	0.93	0.74	0.47	0.96	0.88
Adjusted P trend	0.44	0.17	0.60	0.74	0.20	0.87	0.75

\* Adjusted for race, mother's age, mother's education, gestational age, birth weight, birth length, and parental myopia.

populations, possibly indicating that environmental factors are more important than congenital predispositions.

One of the strengths of our study design is a relatively large, population-based sample. MRI scans in young children are difficult to obtain due in no small part to the need for subject cooperation and parental consent, and our study is the first to provide data on this population. The accuracy of our measurements was partly limited by the acquisition time afforded to us. General limitations include the cross-sectional nature of our study which limits inferences of causation, and the relatively small proportion of myopic children. Although we did not systematically select a subset for analysis, there may also have been unavoidable selection bias as only children whose parents consented underwent MRI shortly after birth. Most of the children had returned home by the time of the MRI, and many parents were unwilling to return to the hospital for their children to undergo the scan. Also, as we did not sedate the babies, many children who were unable to sleep through the scan had to be excluded. Other studies using MRI to analyze eye shape have also had higher resolution images than we had. These are however nondifferential errors that should not affect the relationships we found.

In conclusion, our study has shown that the shape of the newborn eye becomes increasingly prolate with increasing AL, and that most newborn Singaporean Asian children are born with prolate eyes. Race and maternal educational attainment are associated with the size of the eye at birth. The homogeneity of eye shape at birth suggests that it may not influence subsequent refractive development, but a longitudinal study is needed to confirm this.

### Acknowledgments

Supported by National Medical Research Council (NRMC) Grant NMRC/1009/2005 and NMRC/TCR/004-NUS/2008; Agency for Science, Technology and Research (A\*STAR) Grant SICS-09/1/1/001; the Young Investigator Award at the National University of Singapore (NUSYIA FY10 P07); and the National University of Singapore MOE AcRF Tier 1.

Disclosure: **L.S. Lim**, None; **G.H. Chong**, None; **P.T. Tan**, None; **Y.-S. Chong**, None; **K. Kwek**, None; **P.D. Gluckman**, None; **M.V. Fortier**, None; **S.-M. Saw**, None; **A. Qiu**, None

### References

- Lin LL, Shih YF, Tsai CB, et al. Epidemiologic study of ocular refraction among schoolchildren in Taiwan in 1995. *Optom Vis Sci.* 1999;76:275-281.
- Saw SM, Shankar A, Tan SB, et al. A cohort study of incident myopia in Singaporean children. *Invest Ophthalmol Vis Sci.* 2006;47:1839-1844.
- Wong TY, Foster PJ, Hee J, et al. Prevalence and risk factors for refractive errors in adult Chinese in Singapore. *Invest Ophthalmol Vis Sci.* 2000;41:2486-2494.
- Ikuno Y, Sayanagi K, Soga K, et al. Lacquer crack formation and choroidal neovascularization in pathologic myopia. *Retina.* 2008;28:1124-1131.
- Ikuno Y. [Pathogenesis and treatment of myopic foveoschisis]. *Nippon Ganka Gakkai Zasshi.* 2006;110:855-863.
- Ikuno Y, Tano Y. Early macular holes with retinoschisis in highly myopic eyes. *Am J Ophthalmol.* 2003;136:741-744.
- Wong TY, Klein BE, Klein R, Knudtson M, Lee KE. Refractive errors, intraocular pressure, and glaucoma in a white population. *Ophthalmology.* 2003;110:211-217.
- Wong TY, Foster PJ, Johnson GJ, Seah SK. Refractive errors, axial ocular dimensions, and age-related cataracts: the Tanjong Pagar survey. *Invest Ophthalmol Vis Sci.* 2003;44:1479-1485.
- Sect B, Wong TY, Tan DT, et al. Myopia in Singapore: taking a public health approach. *Br J Ophthalmol.* 2001;85:521-526.
- Javitt JC, Chiang YP. The socioeconomic aspects of laser refractive surgery. *Arch Ophthalmol.* 1994;112:1526-1530.
- Lim MC, Gazzard G, Sim EL, Tong L, Saw SM. Direct costs of myopia in Singapore. *Eye.* 2009;23:1086-1089.
- Hammond CJ, Snieder H, Gilbert CE, Spector TD. Genes and environment in refractive error: the twin eye study. *Invest Ophthalmol Vis Sci.* 2001;42:1232-1236.
- Lin LL, Chen CJ. Twin study on myopia. *Acta Genet Med Gemellol (Roma).* 1987;36:535-540.
- Lim IS, Gazzard G, Low YL, et al. Dietary factors, myopia, and axial dimensions in children. *Ophthalmology.* 2010;117:993-997.
- Saw SM, Chua WH, Wu HM, Yap E, Chia KS, Stone RA. Myopia: gene-environment interaction. *Ann Acad Med Singapore.* 2000;29:290-297.
- Saw SM, Wu HM, Hong CY, Chua WH, Chia KS, Myopia Tan D. and night lighting in children in Singapore. *Br J Ophthalmol.* 2001;85:527-528.
- Saw SM, Hong CY, Chia KS, Stone RA, Tan D. Nearwork and myopia in young children. *Lancet.* 2001;357:390.
- Saw SM, Nieto FJ, Katz J, Chew SJ. Distance, lighting, and parental beliefs: understanding near work in epidemiologic studies of myopia. *Optom Vis Sci.* 1999;76:355-362.
- Saw SM, Nieto FJ, Katz J, Schein OD, Levy B, Chew SJ. Factors related to the progression of myopia in Singaporean children. *Optom Vis Sci.* 2000;77:549-554.
- Atchison DA, Pritchard N, Schmid KL, Scott DH, Jones CE, Pope JM. Shape of the retinal surface in emmetropia and myopia. *Invest Ophthalmol Vis Sci.* 2005;46:2698-2707.
- Atchison DA, Jones CE, Schmid KL, et al. Eye shape in emmetropia and myopia. *Invest Ophthalmol Vis Sci.* 2004;45:3380-3386.
- Logan NS, Gilmartin B, Wildsoet CF, Dunne MC. Posterior retinal contour in adult human anisomyopia. *Invest Ophthalmol Vis Sci.* 2004;45:2152-2162.
- Singh KD, Logan NS, Gilmartin B. Three-dimensional modeling of the human eye based on magnetic resonance imaging. *Invest Ophthalmol Vis Sci.* 2006;47:2272-2279.
- Lim IS, Yang X, Gazzard G, et al. Variations in eye volume, surface area, and shape with refractive error in young children by magnetic resonance imaging analysis. *Invest Ophthalmol Vis Sci.* 2011;52:8878-8883.
- Stone RA, Flitcroft DI. Ocular shape and myopia. *Ann Acad Med Singapore.* 2004;33:7-15.
- Ip JM, Huynh SC, Robaei D, et al. Ethnic differences in the impact of parental myopia: findings from a population-based study of 12-year-old Australian children. *Invest Ophthalmol Vis Sci.* 2007;48:2520-2528.
- Zadnik K, Satariano WA, Mutti DO, Sholtz RI, Adams AJ. The effect of parental history of myopia on children's eye size. *JAMA.* 1994;271:1323-1327.
- Edwards MH. Effect of parental myopia on the development of myopia in Hong Kong Chinese. *Ophthalmic Physiol Opt.* 1998;18:477-483.
- Mutti DO, Mitchell GL, Moeschberger ML, Jones LA, Zadnik K. Parental myopia, near work, school achievement, and children's refractive error. *Invest Ophthalmol Vis Sci.* 2002;43:3633-3640.
- Saw SM, Carkeet A, Chia KS, Stone RA, Tan DT. Component dependent risk factors for ocular parameters in Singapore Chinese children. *Ophthalmology.* 2002;109:2065-2071.
- Du J, Younes L, Qiu A. Whole brain diffeomorphic metric mapping via integration of sulcal and gyral curves, cortical surfaces, and images. *Neuroimage.* 2011;56:162-173.

32. Ceritoglu C, Wang L, Selemon LD, Csernansky JG, Miller MI, Ratnanather JT. Large deformation diffeomorphic metric mapping registration of reconstructed 3D histological section images and in vivo MR images. *Front Hum Neurosci.* 2010;4:43.
33. Zhong J, Phua DY, Qiu A. Quantitative evaluation of LDDMM, FreeSurfer, and CARET for cortical surface mapping. *Neuroimage.* 2010;52:131-141.
34. Ishii K, Iwata H, Oshika T. Quantitative evaluation of changes in eyeball shape in emmetropization and myopic changes based on elliptic Fourier descriptors. *Invest Ophthalmol Vis Sci.* 2011;52:8585-8591.
35. Fan DS, Lam DS, Wong TY, et al. The effect of parental history of myopia on eye size of pre-school children: a pilot study. *Acta Ophthalmol Scand.* 2005;83:492-496.
36. Fledelius HC. Pre-term delivery and the growth of the eye. An ophthalmometric study of eye size around term-time. *Acta Ophthalmol Suppl.* 1992;10-15.
37. Isenberg SJ, Neumann D, Cheong PY, Ling YL, McCall LC, Ziffer AJ. Growth of the internal and external eye in term and preterm infants. *Ophthalmology.* 1995;102:827-830.
38. Axer-Siegel R, Herscovici Z, Davidson S, Linder N, Sherf I, Snir M. Early structural status of the eyes of healthy term neonates conceived by in vitro fertilization or conceived naturally. *Invest Ophthalmol Vis Sci.* 2007;48:5454-5458.
39. Cheng HM, Singh OS, Kwong KK, Xiong J, Woods BT, Brady TJ. Shape of the myopic eye as seen with high-resolution magnetic resonance imaging. *Optom Vis Sci.* 1992;69:698-701.
40. Mehra KS, Khare BB, Vaithilingam E. Refraction in full-term babies. *Br J Ophthalmol.* 1965;49:276-277.
41. Ingram RM, Barr A. Changes in refraction between the ages of 1 and 3 1/2 years. *Br J Ophthalmol.* 1979;63:339-342.
42. Lam DS, Fan DS, Lam RF, et al. The effect of parental history of myopia on children's eye size and growth: results of a longitudinal study. *Invest Ophthalmol Vis Sci.* 2008;49:873-876.
43. Saw SM, Chan YH, Wong WL, et al. Prevalence and risk factors for refractive errors in the Singapore Malay Eye Survey. *Ophthalmology.* 2008;115:1713-1719.
44. Pan CW, Wong TY, Lavanya R, et al. Prevalence and risk factors for refractive errors in Indians: the Singapore Indian Eye Study (SINDI). *Invest Ophthalmol Vis Sci.* 2011;52:3166-3173.